Macromolecules

ARTICLE

pubs.acs.org/Macromolecules

Molecular Imaging and Analysis of Branching Topology in Polyacrylates by Atomic Force Microscopy

Sherryl Y. Yu-Su, Frank C. Sun,[†] and Sergei S. Sheiko*

Department of Chemistry, The University of North Carolina at Chapel Hill, Chapel Hill, North Carolina 27599-3290, United States

Dominik Konkolewicz, Hyung-il Lee,[‡] and Krzysztof Matyjaszewski*

Center for Macromolecular Engineering, Department of Chemistry, Carnegie Mellon University, 4400 Fifth Avenue, Pittsburgh, Pennsylvania 15213, United States

Supporting Information

ABSTRACT: Molecular imaging by AFM provides direct and quantitative information about branching topology including length and distribution of branches, not accessible by other methods. In this paper, we report the analysis of branching in linear acrylate-based macromolecules synthesized via free radical polymerization (FRP) and atom transfer radical polymerization (ATRP). The branched structures are formed from chain transfer reactions, specifically transfer to polymer. Quantitative analysis showed that both methods produced branched species, with FRP having degree of branching of 0.035 ± 0.003% and ATRP having a degree of branching of 0.025 ± 0.002%, when measured per backbone repeat unit. The observed lower branching density in ATRP compared to FRP is consistent with a recent ^{13}C NMR study, which also found that controlled radical methods, such as ATRP give lower degrees of branching than FRP. The absolute fraction of long chain branches measured by AFM is significantly lower than the total amount of branches evaluated by measurement of fraction of quaternary carbons using ^{13}C NMR, indicating a predominant intramolecular chain transfer.

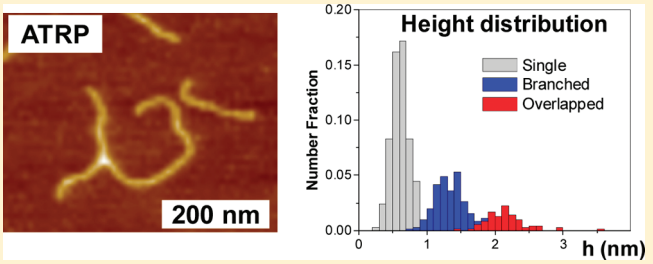

INTRODUCTION

Quantitative information about macromolecular branching topology is vital for the design of materials with desired properties. The information about the distribution and length of branches becomes increasingly valuable as more novel and complex designer structures, such as star- and brush-like macromolecules and dendrimers, are being designed and prepared for micro- and nanoscale devices using various controlled radical polymerization processes.[1] For many applications, the branched structures are deliberately incorporated into the molecules. In general, however, branching occurs spontaneously as a frequent and undesirable side reaction during free radical polymerizations (FRP). Uncontrolled branching as a result of chain transfer to polymer during FRP remains a key industrial issue that persists today since it significantly affects materials properties and performance.[2]

Unlike many polymers such as polyethylene, the branching in polyacrylates was only reported in the last two decades. The initial studies quantified the branching in polyacrylates by measuring the ^{13}C NMR spectrum of poly(*n*-butyl acrylate).[3] In polyacrylates, these branches are typically formed by one of two processes. The first and most prevalent process is the intramolecular backbiting. In this case, the secondary propagating radical abstracts a proton from the same polymer chain, typically three units before the active radical, as illustrated in the top pathway of Scheme 1.[4] This introduces a short chain branch into the polymer, once the tertiary radical propagates. The second process is the intermolecular transfer, wherein a propagating secondary radical attacks a different polymer chain, which results in a dead chain and a newly activated radical placed along the second polymer chain, which after propagation leads to a long chain branch in the second polymer. This is shown in the lower pathway of Scheme 1.[4] The intramolecular, and intermolecular processes represent two ways that a midchain radical can be formed. However, Charleux et al.[5] showed that in many cases, the intramolecular reaction dominates the intermolecular one. Although it is possible to minimize the impact of these transfer reactions on the resulting material,[6] it is not possible to prevent these reactions from occurring.

In addition to propagation from mid chain radicals, the midchain radical may undergo β-scission, yielding a macromonomer which can react with a propagating chain to give a long chain branch (Scheme 2).[4] The formation of a macromonomer followed by side-chain propagation complicates the distinction between a long chain and short chain branching. This is because a midchain radical formed by backbiting can either produce a short chain branch

Received: April 8, 2011
Revised: June 22, 2011
Published: July 08, 2011

Scheme 1. Formation of Short Chain Branches by Back Biting (Top Pathway) and Long Chain Branches by Intermolecular Hydrogen Abstraction (Lower Pathway)[a]

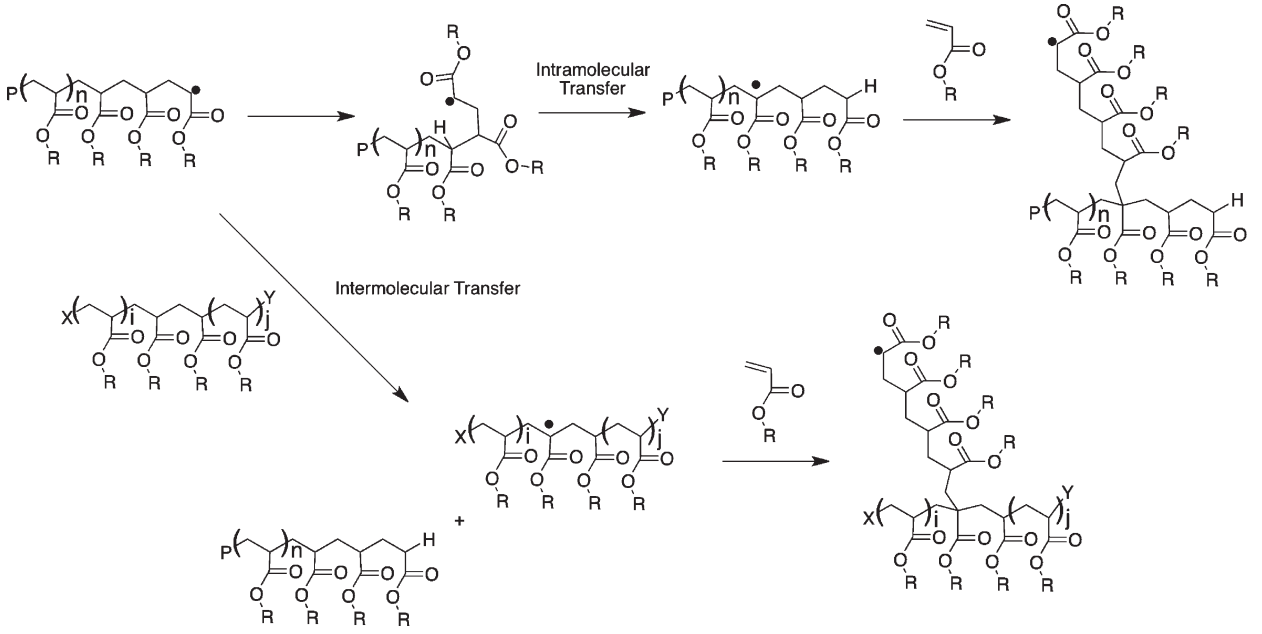

[a] Y represents the capping agent in controlled radical polymerization, e.g. halogen in ATRP or nitroxide in nitroxide mediated polymerization (NMP), or an end-group in FRP. X and P represent initiating sites or initiator fragments.

Scheme 2. Process of β-Scission, Which Can Result in a Long Chain Branch, by Propagation of the Resulting Macromonomer[a]

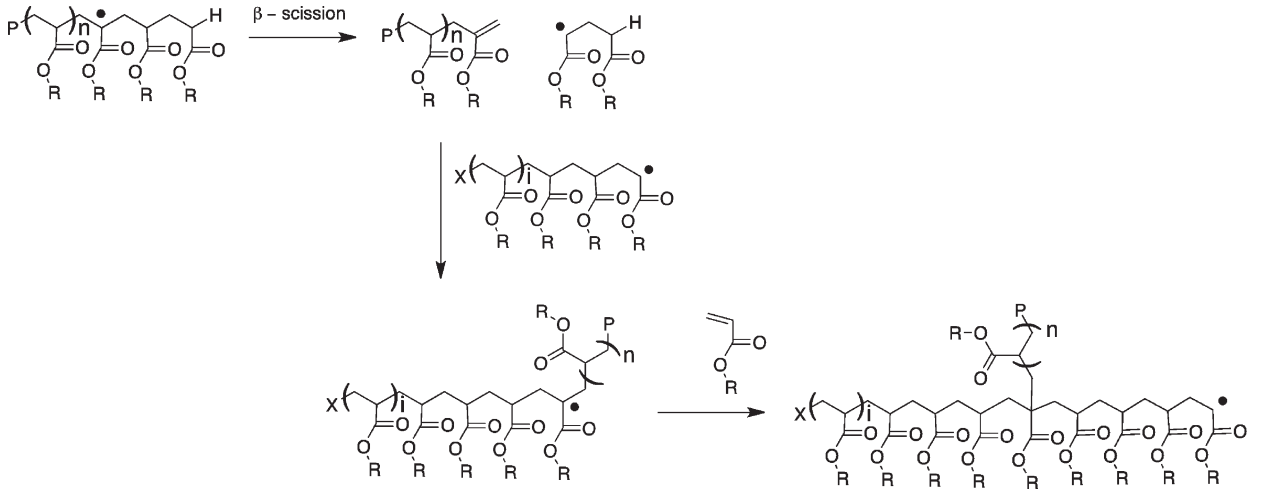

[a] X and P represent initiating sites or initiator fragments.

(typical scenario) or undergo β-scission followed by incorporation of the macromonomer into a second polymer chain. The second product is indistinguishable from a long chain branching event, which suggests that any measure for long chain branches is actually an upper limit on the number of branches formed by intermolecular transfer.

The advent of controlled radical polymerization (CRP) methods has greatly impacted polymer synthesis, by providing simple routes for the creation of well-defined polymers and complex architectures.[1h,7] In particular, atom transfer radical polymerization (ATRP) is frequently used for the synthesis of various polymers with well-defined molecular weights, with very narrow molecular weight distributions, indicating that very few chain transfer or termination reactions occurred during the polymerization.[7b] This is due to the fact that, at any given time, only a small fraction of the polymer chains are actively propagating, while majority are in a halogen-capped dormant state.[7b] Nevertheless, there is evidence of chain transfer reactions during acrylate ATRP, resulting in randomly branched structures, reminiscent of FRP products.[8] This is due to the free radical nature of the propagating species in ATRP, which can undergo the same transfer reactions as in FRP.[9]

Despite the presence of branches in polymers synthesized by ATRP and other CRP methods, a recent report found that the extent of branching is significantly lower in CRP methods, including ATRP, than in their FRP analogues.[10] In this case,

the branching levels were measured by ^{13}C NMR spectroscopy, and showed that the concentration of branches was appreciably lower in a CRP system than in a FRP polymerization. In that study, the results were explained by a higher reactivity of short radicals that are present in high concentrations in FRP systems, in contrast to longer chain radicals (prevalent) in CRP systems. In a subsequent theoretical study, Reyes and Asua[11] proposed that the decrease in branches in CRP compared to FRP is due to the short transient radical lifetime in CRP, which decreases the likelihood of branching events in CRP. With the ongoing debate about the cause of the lower degree of branching in CRP, it is of interest to quantify the exact amount of branching and the nature of branches present.

Characterization of a branched polymer architecture includes the branching density, the distribution of branches along the chain, and the distribution of branch lengths.[2c,f,12] The techniques commonly used for branching analysis include ^{13}C NMR spectroscopy, rheology, size exclusion chromatography (SEC) coupled with multiangle laser light scattering (SEC−MALLS) and intrinsic viscosity measurements (SEC−Visc). However, there are inherent limitations and discrepancies between these methods, making it difficult to draw general conclusions about the branching distribution and length of branches both of which directly affect structure−property relationships of polymeric materials. For instance, ^{13}C NMR is a straightforward method that has been used extensively to study branching in polyethylene[2c,13] and other common polymers.[14] However, the low natural abundance of ^{13}C isotope results in poor sensitivity and low resolution of peaks.[13h,i] More importantly, ^{13}C NMR is unable to distinguish beyond branches containing $\geq C_6$[13g,i,15] (perhaps longer if solid-state NMR is used but with caveats).[13i,16] Resolution enhancement is possible but with limited results,[13i] and there have been recent reports of melt state ^{13}C NMR used to obtain improved quantification of the number of branches.[17] Another way to detect branches is to study rheological properties that exhibit strong sensitivity to branching. This indirect approach also has several drawbacks, such as sample preparation issues, the need for physical models, difficulty in determining zero-shear viscosity η_0 for some materials,[13h,18] and its insensitivity to short chain branching (SCB) as it detects only long chain branches that are longer than the entanglement strand.[13g,i,18] This definition of a long chain branching (LCB) is quite different from the ^{13}C NMR definitions. Both ^{13}C NMR and rheology give an average branch value for the material despite this inconsistency. In contrast, triple-detector SEC provide information about the distribution of branching across the whole molecular weight spectrum, and is a good analytical technique for high molecular weight samples.[2c,13h,19] Using a combination of SEC−MALLS and SEC−Visc generates a Mark−Houwink plot, which gives information about LCB via a slope change, and SCB, which produces a shift in the curve but no slope change when compared to a linear standard.[2c] However, some assumptions must be made in order to obtain this information, which can lead to erroneous conclusions about the degree of branching in a molecule.[13h] For SEC−MALLS, the radius of gyration can be directly used to determine the degree of branching at that molar mass, that is, unlike the triple-detector SEC method, no assumptions about molecular interactions are needed.[19b] Nonetheless, there are shortcomings to this technique, such as the abnormal elution of highly branched species,[13h,19a,19b] and the fact that both SEC methods can give large errors at very low LCB levels.[13g,h,15]

Imaging of individual molecules by an atomic force microscope (AFM) can resolve the above issues, as it allows quantitative analysis of both distribution and length of branches along the backbone. In addition, one obtains various molecular dimensions such as molecular weight,[20] contour length, radius of gyration, fractal dimension, persistence length,[21] as well as information about the conformational transitions of polymers,[22] supramolecular self-assembly,[23] and branching data.[21c,24] Thus, by using molecular imaging, one can directly confirm and characterize the branching topology.

This paper presents direct evidence obtained from molecular visualization experiments that branching by chain transfer to polymer occurs during acrylate polymerization via ATRP and FRP. In addition, a comparison between acrylate and methacrylate-based macromolecules synthesized by ATRP is shown. A preliminary analysis of the degree of branching of each molecule was performed. To facilitate the molecular visualization and analysis, poly(2-(trimethylsilyloxy)ethyl acrylate) (PHEA-TMA) synthesized by ATRP and FRP were converted into macroinitiators, poly(2-(2-bromopropionyloxy)ethyl acrylate) (PBPE) and subsequently decorated with poly(*n*-butyl acrylate) (PBA) side chains, creating macromolecules that are easily imaged and analyzed by AFM. The enhancement of the height contrast due to the side chains is similar to that of linear chains decorated with bulky molecules[25] and nanoparticles.[26]

EXPERIMENTAL PART

Materials and Methods. All chemicals were purchased from Aldrich or Acros, and used as received unless otherwise stated. 2-Hydroxyethyl acrylate (HEA) and *n*-butyl acrylate were purchased from Acros and distilled under vacuum prior to use. *N*,*N*,*N*′,*N*″,*N*″-pentamethyldiethylenetriamine (PMDETA), dimethyl 2,6-dibromoheptanedioate (97%) (DMDBH), 2-bromopropionyl bromide (98%), ethyl 2-bromoisobutyrate (98%) (EBiB), triethylamine (98%) were used as received. CuBr was purified as described previously. 2-(trimethylsilyloxy)ethyl acrylate (HEA-TMS) was distilled under vacuum prior to use. The synthesis of backbones and corresponding molecular brushes via ATRP and FRP are presented in Supporting Information.

The average molecular weights and molecular weight distributions of the backbone polymers and the subsequent brushes were measured by size exclusion chromatography (SEC) equipped with Waters microstyragel columns (pore size 10^5, 10^4, 10^3 Å) coupled with a multiangle laser light-scattering (MALLS) detector (Wyatt, DAWN EOS, $\lambda = 690$ nm). d*n*/d*c* of the poly(alkyl acrylate) chains was determined from refractive index measurements on a series of solutions (∼0.1−1.0 mg/mL in THF) using an Abbe Refractometer NAR-1T from Atago USA, Inc.) (d*n*/d*c* = 0.045 mL/g). The accompanying software to the SEC−MALLS (Astra) was used to determine radii of gyration and calculate the branch ratio for the backbones relative to linear poly(methyl methacrylate) (PMMA) (M_n = 460 000 g/mol, d*n*/d*c* = 0.086 mL/g) (American Polymer Standards Corp.).[27] Monomer conversion was determined by gas chromatography (GC) using a Shimadzu GC 14-A gas chromatograph equipped with a FID detector and ValcoBond 30 m VB WAX Megabore column.

Single molecule films were prepared by spincasting dilute chloroform solutions (∼0.01%wt.) onto freshly cleaved mica (Laurell Technologies Corp. Model WS-400A-6NPP/Lite). Dense films were prepared using the Langmuir−Blodgett trough (KSV 5000 Instrument equipped with a trough and barriers made of PTFE and a Wilhemy plate balance, Milli-Q double-distilled water $\rho = 18.2$ MΩ). The polymer film was transferred to freshly cleaved mica at a controlled low pressure of 0.5 mN/m. The same procedure was used for the preparation of films of each polymer brush encapsulated in a matrix of linear poly(*n*-butyl acrylate).

All of the films were imaged using a Multimode Atomic Force Microscope in tapping-mode from Veeco Metrology group equipped with a Nanoscope IIIA controller and silicon cantilevers with resonance frequencies of about 160 kHz, spring constants of 5.0 N/m, and radii less

Scheme 3. Synthetic Route for a Molecular Brush Consisting of a Poly(alkyl (meth)acrylate)-Based Backbone (X) and PBA Side Chains Grafted from Each Monomer Unit of the Backbone via ATRP, Giving the Brush Polymer (Y)

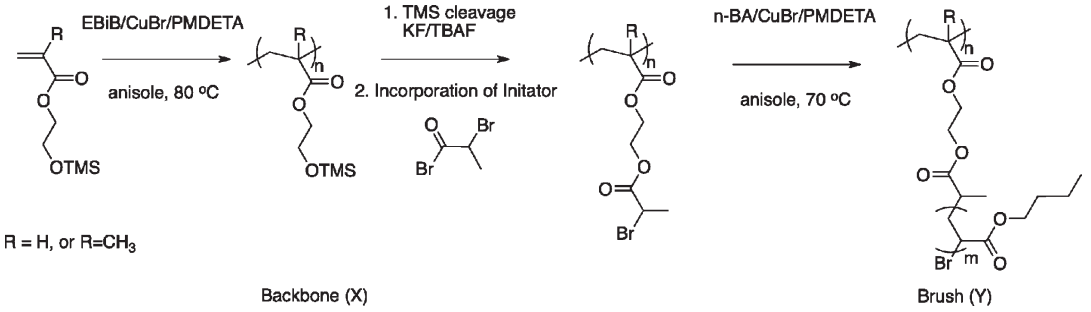

Table 1. Reaction Conditions and Characterization of the PBA Brush Copolymers

	formula	polymerization method	monomer	DP[a]	M_n[b] (10^3)	PDI[b]
A-C$_X$	PHEA-TMS$_{1,000}$	ATRP	HEA-TMS	1010[b]	190	1.6
A-C$_Y$	P(BPE$_{1,000}$-*g*-PBA$_{35}$)	ATRP	*n*-BA	35[c]	7460	1.48
A-F$_X$	PHEA-TMS$_{1,040}$	FRP	HEA-TMS	1040[b]	196	3.86
A-F$_Y$	P(BPE$_{1,040}$-*g*-PBA$_{45}$)	ATRP	*n*-BA	45[c]	1330	3.28
M-C$_X$	PHEMA-TMS$_{1,600}$	ATRP	HEMA-TMS	1630[b]	330	1.11
M-C$_Y$	P(BPEM$_{1,600}$-*g*-PBA$_{25}$)	ATRP	*n*-BA	25[c]	4400	1.09

[a] Calculated from M_n/m_0, where M_n = molar mass obtained from GPC−MALLS, m_0 = molar mass of monomer (m_0 = 188 g/mol for HEA-TMS and m_0 = 202 g/mol for HEMA-TMS). [b] Obtained from GPC−MALLS in THF. [c] Obtained from gravimetry.

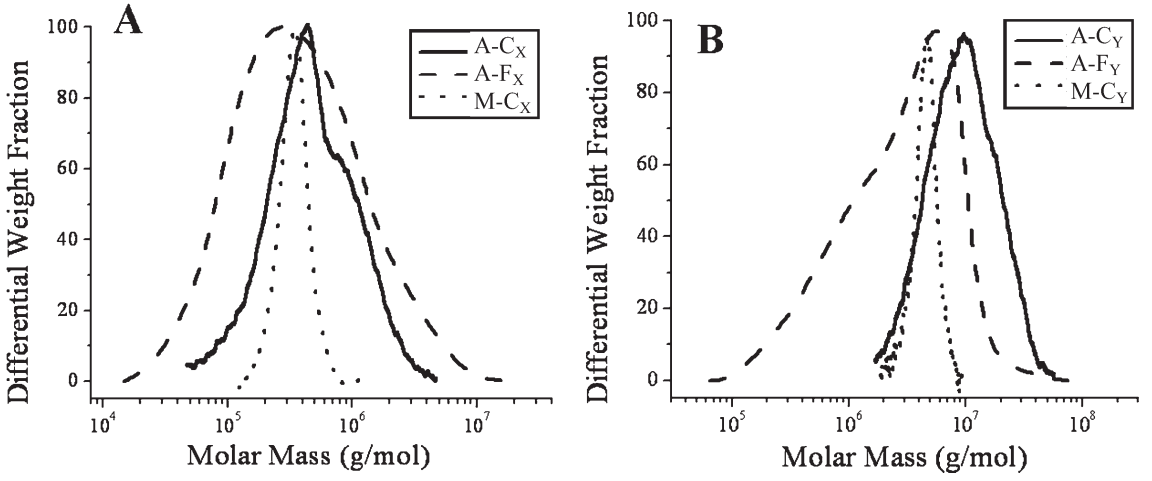

Figure 1. SEC−MALLS traces of the (A) backbones (X) and (B) their corresponding PBA brushes (Y). The reactions carried out using ATRP were better controlled, than the FRP synthesized polymers. A high molecular weight shoulder in the poly(alkyl acrylate) backbone synthesized by ATRP, may be caused by branched or coupled species. (**A-C$_X$** and **A-C$_Y$**, acrylate ATRP backbone and brush; **A-F$_X$** and **A-F$_Y$**, acrylate FRP backbone and brush; **M-C$_X$** and **M-C$_Y$**, methacrylate ATRP backbone and brush).

than 10 nm. Specially developed computer software was used for length measurements from the captured micrographs.

RESULTS AND DISCUSSION

Characterization by SEC. Various polymer backbones and brushes were synthesized, following the general principles outlined in Scheme 3. The only exception is one sample where the backbone was synthesized under free radical polymerization conditions, rather than under ATRP conditions (see Supporting Information for details). A nomenclature is introduced to describe these polymers, for example **M-C$_X$** which refers to a methacrylic (M) backbone only (X) synthesized under controlled (C) or ATRP conditions. In this way **A-F$_Y$** refers to a brush(Y) with acrylic backbone synthesized under free radical (F) conditions. Initially, poly(2-hydroxyethyl acrylate) (PHEA) backbones with comparable degrees of polymerization *N* were

dx.doi.org/10.1021/ma200821a |*Macromolecules* 2011, 44, 5928–5936

synthesized, one via atom transfer radical polymerization (ATRP) (**A-C$_x$**) and the other by free radical polymerization (FRP) (**A-F$_X$**). Note that the conversion in samples **A-C$_X$** and **A-F$_X$** are similar. The degree of branching varies with conversion, particularly at high conversion, however, the conversions of 40% and 50% are sufficiently low and similar that they should not introduce significant differences in branching due to the conversion alone.[10] Both were subsequently converted into macroinitiators and decorated with poly(*n*-butyl acrylate) (PBA) side chains to give molecular brushes (**A-C$_Y$** and **A-F$_Y$**) using the "grafting-from" ATRP method. In addition, a brush (**M-C$_Y$**) consisting of a poly(2-hydroxyethyl methacrylate) (PHEMA) backbone (**M-C$_X$**) and PBA side chains was synthesized using ATRP. The reaction route is presented in Scheme 1 with initial characterization results for the three brushes summarized in Table 1.

The SEC−MALLS traces for the backbones (**A-C$_X$**, **A-F$_X$**, **M-C$_X$**) and the corresponding brushes (**A-C$_Y$**, **A-F$_Y$**, **M-C$_Y$**) are shown in Figure 1. As expected, the backbones **A-C$_X$** and **M-C$_X$**, synthesized by ATRP, are better controlled and have lower polydispersity indices (PDI) than the FRP-synthesized backbone **A-F$_X$**.[7b,28] There is a high molecular weight shoulder present in the acrylate backbone trace **A-C$_X$**, which is likely to be due to transfer and termination side reactions.[19b,29] On the other hand, the broad SEC−MALLS trace observed for **A-F$_X$** corroborates numerous studies by others that FRP-made poly(alkyl acrylates) are highly polydisperse.[14,30] Noteworthy is the fact that the trace observed for **M-C$_X$**, the methacrylate-based backbone, is significantly narrower than both **A-C$_X$** and **A-F$_X$**. This is attributed to the absence of easily abstractable hydrogens in the backbone that can participate in chain transfer reactions.

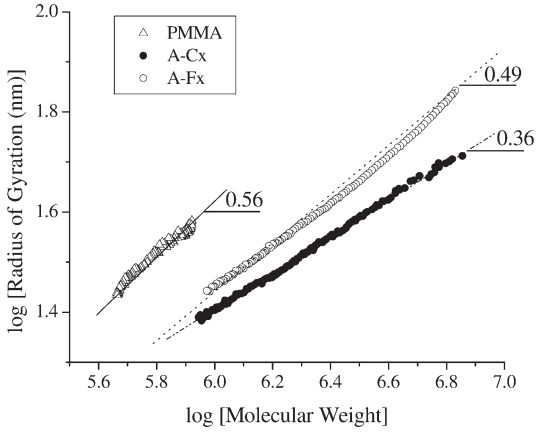

Figure 2. Log−log plot of the radius of gyration ($R_g \sim M^{\nu}$) vs molecular weight (M) of poly(alkyl acrylate) backbones synthesized via ATRP (**A-C$_X$**) and FRP (**A-F$_X$**). The corresponding scaling exponents ν (slopes of the lines) are less than the Flory exponent ($\nu \cong 0.6$) for a linear chain in a good solvent, as observed for a reference sample of linear PMMA with M^n = 460 000.

Subsequent grafting of PBA side chains from each backbone was successful, as evidenced by the shift to higher molecular weights (Figure 1B). The brush traces obtained have similar characteristics to their respective backbones, such that **A-C$_Y$** and **M-C$_Y$** peaks are narrower than that of **A-F$_Y$**. There is still a slight shoulder present in the high molecular weight region of the **A-C$_Y$** curve, reflecting the backbone characteristic. The trace for **A-F$_Y$** is still very broad, with emphasis on the lower molecular weight region, as expected for FRP.

SEC−MALLS is a conventional method for branching characterization through the conformation plot log R_g vs log M_n. Figure 2 shows the measured log R_g (log M_n) plots for the brush backbones (**A-C$_X$** and **A-F$_X$**) and a linear PMMA (M_n = 460 000) along with the corresponding slope values. The PMMA-460k sample is used here as a reference sample to illustrate the deviation from linear polymer behavior in a good solvent since there is no exact standard available for the poly(alkyl acrylate) backbones. The slope of PMMA-460k (ν = 0.56 ± 0.01) is consistent with Flory model for a linear chain under good solvent conditions (ν = 0.6).[31] For **A-C$_X$** and **A-F$_X$** backbones, the slopes (ν = 0.36 ± 0.01 and ν = 0.49 ± 0.01, respectively) are considerably below the expected ν = 0.6 exponent and hence indicate branched structures. SEC−MALLS, however, does not give information about the shape of the branched macromolecules.

The presence of branches in the ATRP synthesized poly(alkyl acrylate) backbone (**A-C$_X$**) is consistent with ^{13}C NMR data as seen in literature reports.[3,10,17]

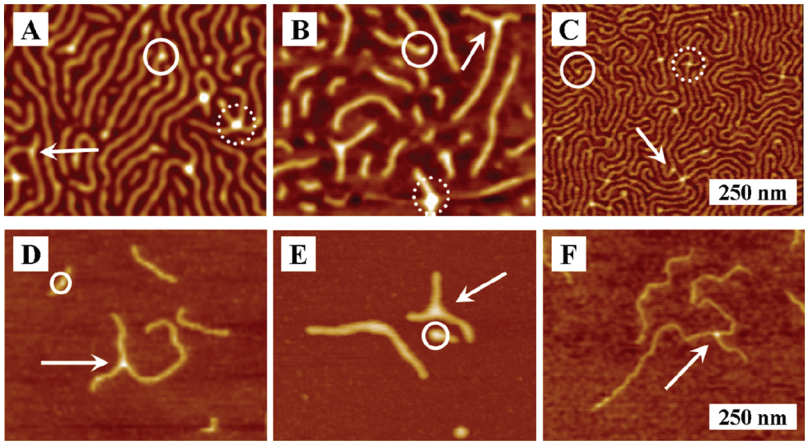

Figure 3. AFM images of PBA brushes made from poly(alkyl acrylate) and poly(alkyl methacrylate) backbones. From the dense films above (A, **A-C$_Y$**; B, **A-F$_Y$**; C, **M-C$_Y$**), one can see linear, long branched chains (arrows), chains with knots that are believed to be short branches (solid circle), and what appear to be overlapping linear chains (dotted circle) present in all of the samples. The density of each film is affected by the width of the brushes; i.e., **M-C$_Y$** has the narrowest width at 21 nm and **A-F$_Y$** the widest at 70 nm. Further evidence for the presence of branched macromolecules is provided by the AFM images of each brush polymers embedded in linear PBA matrix (white arrows pointing to branch junctions). [D, **A-C$_Y$**; E, **A-F$_Y$**; F, **M-C$_Y$**].

Molecular Imaging and Characterization of Macromolecules by AFM. To find additional evidence for branching, molecular imaging by AFM was employed. Height micrographs in Figure 3 show individual brush-like macromolecules of **A-C$_Y$**, **A-F$_Y$**, and **M-C$_Y$** that were clearly resolved both within dense monolayers (Figure 3A−C) and as single species (Figure 3D−F). The molecular resolution is assisted by the strong topographic contrast between the surface and the molecule as a result of desorbed side chain segregation atop the backbone.[32] In addition to the contrast enhancement, the adsorbed side chains separate individual molecules and cause extension of the backbone. Thus, all of these factors combined facilitate molecular imaging and quantitative analysis of molecular dimensions and branching topology.[1a−c]

More than 300 molecules for each sample were measured to obtain representative length distributions (Figure 4). Table 2 summarizes the data of the analysis of length distribution. The obtained data clearly prove that molecules **A-C$_Y$** and **M-C$_Y$** are better defined than **A-F$_Y$**. The ATRP synthesized samples **A-C$_Y$** and **M-C$_Y$** demonstrate significantly narrower length distribution, when compared to the FRP sample **A-F$_Y$**. In agreement with the SEC−MALLS data in Table 1 and Figure 1a, the **M-C$_Y$** distribution is narrower than that of **A-C$_Y$**. The calculated PDI = $M_w/M_n = L_w/L_n$ for **A-F$_Y$** based on molecular imaging analysis is lower than that obtained from SEC−MALLS. This is attributed to the particular broadness of the length distribution that requires a much large ensemble of molecules for accurate image analysis.

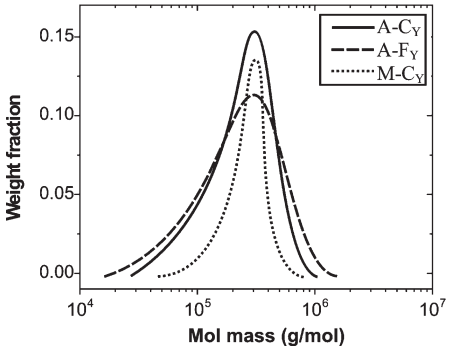

Figure 4. Molecular weight distributions of poly(alkyl acrylate) and poly(alkyl methacrylate)-based PBA brushes (**A-C$_Y$**, **A-F$_Y$**, and **M-C$_Y$**) were obtained from the AFM measurements of molecular contour length. The distributions are reflective of the SEC−MALLS traces of the corresponding macroinitiators (**A-C$_X$**, **A-F$_X$**, and **M-C$_X$**) presented in Figure 1a. In addition, one can conclude that side reactions, such as termination and transfer, dominate **A-F$_Y$**. On the other hand, the molecules in **A-C$_Y$** and **M-C$_Y$** were produced in a more controlled fashion, and yet, one can see that the distribution for **A-C$_Y$** is not as sharply defined as **M-C$_Y$**, which is likely to be due to side reactions during the polymerization.

The observed variations in length distribution are consistent with the molecular length averages. For the poly(alkyl acrylate) and poly(alkyl methacrylate) ATRP samples **A-C$_Y$** and **M-C$_Y$** the measured number-average lengths (L_n = 240 ± 10 nm and 440 ± 10 nm) of the imaged macromolecules agree well with the expected contour length ($L_{n,theo}$ = 252 nm and $L_{n,theo}$ = 407 nm) calculated as $L_{n,theo}$=DP × 0.25 nm, where DP is the number-average degree of polymerization of the backbone (Table 1) and l_0 = 0.25 nm is the length of the monomeric unit. The small discrepancy of 10% in the methacrylate is most likely due to the uncertainties in the molecular weight measured by SEC. The number-average contour length of sample **A-F$_Y$** (L_n = 115 ± 9 nm) is shorter than expected ($L_{n,theo}$= 260 nm). This large deviation is observed for **A-F$_Y$**, is most likely due to the ill defined distribution obtained by uncontrolled polymerization, which again highlights the shortcomings of FRP.

Degree of Branching Analysis by AFM. From cursory inspection of the AFM images, one readily detects three different molecular topologies present in both **A-C$_Y$** and **A-F$_Y$** and to a significantly lesser extent in **M-C$_Y$** of the samples: linear, branched, both very long chain branches and shorter branches, and overlapping linear chains (Figure 3A−C). To ensure that the branches observed were indeed chemically formed structures, brush molecules were purposely diluted with linear PBA (10/90 wt/wt %), which is a good solvent for the PBA brushes (Figure 3D−F). The excluded volume repulsion between the encapsulated brushes results in the extended conformation of brush backbones, while further separating individual molecules from each other.[33] Such methodology reduces the number of physically overlapping entities in a controllable way, ensuring that the branched structures observed are a result of chemical linkages. As can be seen in Figure 3D−E, it is clear that there are indeed randomly branched, predominantly T-shaped, molecules of chemical origin present in **A-C$_Y$** and **A-F$_Y$**. In addition to long chain branches (LCB), one can also see shorter branches, manifested as knots along the backbone.

The assignment of the different topologies present was corroborated by the distribution of the heights of linear chains versus branch junctions of the T-shaped molecules and knots present along the backbone. The thicknesses of the overlapping macromolecules is >2× the height of a linear chain due to a strong difference in wetting properties of an underlying macromolecule and a bare mica substrate. On the basis of the height data, molecules in each dense monolayer film were sorted into three groups and categorized as linear, branched, or overlapping linear chains (Figure 5). From the data, the degree of branching was determined and summarized in Table 2.

Figure 5 shows that majority of the species present for all brushes are linear molecules with a small fraction of overlapping chains. For the poly(alkyl methacrylate)-based sample **M-C$_Y$** made by ATRP (Figure 3F), practically all the molecules are linear chains with very few branched entities, which is because

Table 2. Summary of Length and Branching Analysis Results for Poly(alkyl acrylate) and Poly(alkyl methacrylate)-Based PBA Brush Polymers

	L_n (nm)[a]	PDI[b]	d (nm)[c]	$10^{-6}M_n$[d]	$\lambda \times 10^4$ (nm^{-1})[e]	λ_b (%)[f]	$\beta = 1/\lambda_b$[g]
A-C$_Y$	240 ± 10	1.4 ± 0.2	40 ± 2	9 ± 1	9.9 ± 0.7	0.025 ± 0.002	4000 ± 300
A-F$_Y$	115 ± 9	1.9 ± 0.6	70 ± 4	2 ± 1	14 ± 1	0.035 ± 0.003	2900 ± 300
M-C$_Y$	440 ± 10	1.1 ± 0.2	21 ± 1	3 ± 1	1.1 ± 0.1	0.0028 ± 0.0003	36000 ± 4000

[a] Number-average contour length. [b] Dispersity index, L_w/L_n. [c] Brush width. [d] Obtained from AFM-LB technique.[20] [e] Number of branches per unit length. [f] Percent of branches per repeat unit $\lambda_b = \lambda \times 0.25$ nm and given as percentage. [g] Number of backbone repeat units per branch.

dx.doi.org/10.1021/ma200821a |*Macromolecules* 2011, 44, 5928–5936

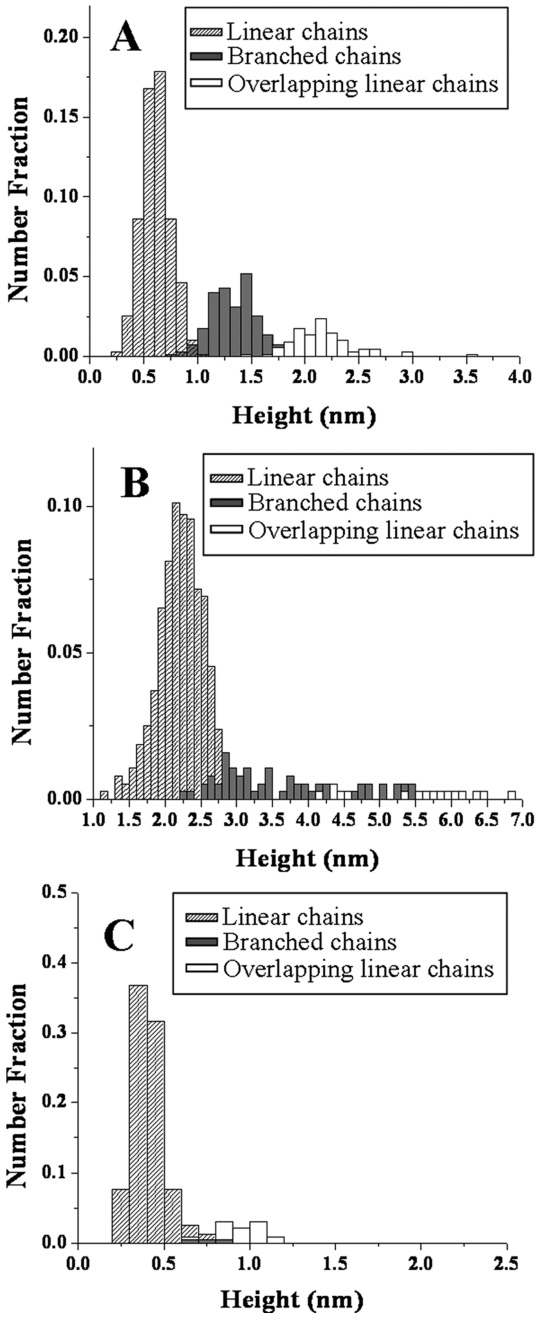

Figure 5. Height distributions correspond to the distribution in topologies present in poly(alkyl acrylate) and poly(alkyl methacrylate)-based brushes. Majority of the imaged molecules are linear chains. Smaller fractions of the higher features correspond to chemically branched and physically overlapped macromolecules. Evidently, both (A) **A-C$_Y$** and (B) **A-F$_Y$** have more branched structures compared to more linear chains in (C) **M-C$_Y$**.

methacrylates do not have an available tertiary hydrogen for chain transfer to polymer.[14,30a] Disproportionation reactions resulting in macromonomers that could be copolymerized with the linear growing chains and traces of impurities in the methacrylate monomer are the possible causes for the branching observed in poly(alkyl methacrylates).[7a]

In the case of poly(alkyl acrylate)-based samples, the occurrence of random branching in acrylates (**A-C$_Y$** and **A-F$_Y$**) is expected regardless of the polymerization technique, with these branches formed by the intermolecular transfer, intramolecular transfer processes, or β-scission at higher reaction temperatures.[7a,30a,34] Quantification of the degree of branching shows that the backbones synthesized by ATRP (**A-C$_Y$**) are less branched than their FRP synthesized counterpart (**A-F$_Y$**) (a degree of branches equal to 0.035% for FRP versus 0.025% for ATRP). This decrease of branching density of ~30% in ATRP compared to FRP agrees well with the ^{13}C NMR experiments which showed similar decreases in overall branching density (inter and intramolecular) in a CRP system, compared to a FRP system.[10] Results are summarized in Table 2.

These results correspond to approximately 20% of molecules in **A-C$_Y$** having a branch point, which seems high initially, however, the polymers have high degrees of polymerization in the backbone, therefore the probability of any one molecule being branched is quite high. In addition, there are also issues due to the limited statistics of molecular imaging. Despite these statistical limitations, the molecular imaging experiments show that the degree of branching is appreciably lower in ATRP than FRP. The 30% decrease in branching in ATRP is much greater than what could be anticipated by the different slightly lower conversion when backbone was prepared by ATRP. It is also important to note that the values of these AFM measured branching fractions for FRP of acrylates are in the order of 0.04%, which is approximately 1 order of magnitude below the total fraction of branches of 0.4% predicted for FRP, at approximately 50% conversion.[10] This discrepancy is likely to be due to the fact that AFM is an excellent method of measuring long chain branches, yet fails detecting short chain branches. In this particular case, AFM suggests that >90% of branches are due to short chain backbiting and propagation, and <10% longer chain branching, which is consistent with literature observations that the majority of branches are caused by intramolecular transfer.[5] Nonetheless, these AFM data, along with other methods such as NMR, suggest that the CRP process itself is responsible for the lower degrees of branching in CRP compared to FRP. The AFM data serve as a direct experimental evidence of the presence and extent of branching in polyacrylates.

CONCLUSIONS

Molecular imaging of branching in linear poly(alkyl acrylate)-based macromolecules synthesized by ATRP and FRP was carried out using a combination of techniques, including molecular imaging by AFM. In agreement with SEC−MALLS measurements, AFM reveals well-defined molecules in the ATRP-made brush polymers (**A-C$_Y$** and **M-C$_Y$**) and poorly defined molecules in the FRP sample (**A-F$_Y$**). Quantification of the degree of branching was achieved through this direct method. Interestingly, the AFM studies indicate that the degree of long chain branching in polyacrylate prepared by ATRP is 0.025 ± 0.002% whereas for polyacrylate prepared by FRP, the degree of long chain branching is 0.035 ± 0.003%. This corresponds to a 30% decrease in the degree of branching in ATRP compared to FRP, which is in excellent agreement with the overall branching measured by ^{13}C NMR. AFM also indicates that long chain branching comprises <10% overall branching, by comparison with ^{13}C NMR data.

Branching analysis by AFM via direct visualization and verification of molecular topology enables branch quantification, both average branch values and branch distribution across

lengths/molecular weight. Since AFM cannot measure very short chain branches, it provides unique possibility to evaluate exclusively LCB and it is a very complementary technique to ^{13}C NMR that can evaluate overall fraction of branches.

■ ASSOCIATED CONTENT

Supporting Information. Additional synthetic procedures. This material is available free of charge via the Internet at http://pubs.acs.org/.

■ AUTHOR INFORMATION

Corresponding Author

*E-mail: (S.S.) sergei@email.unc.edu; (K.M.) km3b@andrew.cmu.edu.

Present Addresses

[†]Johnson & Johnson CPPW, 199 Grandview Road, Skillman, NJ 08558

[‡]Department of Chemistry, University of Ulsan, 93 Daehak-ro, Nam-gu, Ulsan, 680−749, Korea

■ ACKNOWLEDGMENT

We thank Andrew Brown for SEC−MALLS equipment setup and Alper Nese for fruitful discussions. We gratefully acknowledge support from NSF DMR 09-69301 and DMR 09-06985.

■ REFERENCES

(1) (a) Sheiko, S. S.; Moller, M. *Chem Rev* **2001**, *101*, 4099–4123. (b) Zhang, M.; Mueller, A. H. E. *J. Polym. Sci, Part A: Polym. Chem.* **2005**, *43*, 3461–3481. (c) Bannister, I.; Billingham, N. C.; Armes, S. P.; Rannard, S. P.; Findlay, P. *Macromolecules* **2006**, *39*, 7483–7492. (d) Matyjaszewski, K.; Tsarevsky, N. V. *Nature Chem.* **2009**, *1*, 276–288. (e) Gao, H.; Matyjaszewski, K. *Prog. Polym. Sci.* **2009**, *34*, 317–350. (f) Lee, H.-i.; Pietrasik, J.; Sheiko, S. S.; Matyjaszewski, K. *Prog. Polym. Sci.* **2010**, *35*, 24–44. (g) Sheiko, S. S.; Sumerlin, B. S.; Matyjaszewski, K. *Prog. Polym. Sci.* **2008**, *33*, 759–785. (h) Braunecker, W. A.; Matyjaszewski, K. *Prog. Polym. Sci.* **2007**, *32*, 93–146. (i) Liu, F.; Urban, M. W. *Prog. Polym. Sci.* **2010**, *35*, 3–23. (j) Xu, F. J.; Neoh, K. G.; Kang, E. T. *Prog. Polym. Sci.* **2009**, *34*, 719–761. (k) Jang, W.-D.; Kamruzzaman Selim, K. M.; Lee, C.-H.; Kang, I.-K. *Prog. Polym. Sci.* **2009**, *34*, 1–23.

(2) (a) Fetters, L. J.; Kiss, A. D.; Pearson, D. S.; Quack, G. F.; Vitus, F. J. *Macromolecules* **1993**, *26*, 647–654. (b) Jackson, C.; Chen, Y.; Mays, J. W. *J. Appl. Polym. Sci.* **1996**, *59*, 179–188. (c) Wood-Adams, P. M.; Dealy, J. M.; deGroot, A. W.; Redwine, O. D. *Macromolecules* **2000**, *33*, 7489–7499. (d) Ahmad, N. M.; Lovell, P. A.; Underwood, S. M. *Polym. Int.* **2001**, *50*, 625–634. (e) Garcia-Franco, C. A.; Harrington, B. A.; Lohse, D. J. *Macromolecules* **2006**, *39*, 2710–2717. (f) McKee, M. G.; Elkins, C. L.; Park, T.; Long, T. E. *Macromolecules* **2005**, *38*, 6015–6023. (g) Staudinger, U.; Weidisch, R.; Zhu, Y.; Gido, S. P.; Uhrig, D.; Mays, J. W.; Iatrou, H.; Hadjichristidis, N. *Macromol. Symp.* **2006**, *233*, 42–50.

(3) Lovell, P. A.; Shah, T. H.; Heatley, F. *Polym. Commun.* **1991**, *32*, 98–103.

(4) Junkers, T.; Barner-Kowollik, C. *J. Polym. Sci, Part A: Polym. Chem.* **2008**, *46*, 7585–7605.

(5) Farcet, C. l.; Belleney, J. l.; Charleux, B.; Pirri, R. *Macromolecules* **2002**, *35*, 4912–4918.

(6) Junkers, T.; Koo, S. P. S.; Davis, T. P.; Stenzel, M. H.; Barner-Kowollik, C. *Macromolecules* **2007**, *40*, 8906–8912.

(7) (a) Moad, G.; Solomon, D. H.; Moad, G. In *The chemistry of radical polymerization*; Elsevier: Amsterdam and Boston, MA, 2006; p 639; (b) Matyjaszewski, K.; Xia, J. *Chem. Rev.* **2001**, *101*, 2921–2990. (c) Hawker, C. J.; Bosman, A. W.; Harth, E. *Chem. Rev.* **2001**, *101*, 3661–3688. (d) Perrier, S.; Takolpuckdee, P. *J. Polym. Sci, Part A: Polym. Chem.* **2005**, *43*, 5347–5393. (e) Tsarevsky, N. V.; Matyjaszewski, K. *Chem. Rev.* **2007**, *107*, 2270–2299. (f) di Lena, F.; Matyjaszewski, K. *Prog. Polym. Sci.* **2010**, *35*, 959–1021.

(8) (a) Bednarek, M.; Biedron, T.; Kubisa, P. *Macromol. Chem. Phys.* **2000**, *201*, 58–66. (b) Roos, S. G.; Müller, A. H. E. *Macromol. Rapid Commun.* **2000**, *21*, 864–867. (c) Huang, J.; Pintauer, T.; Matyjaszewski, K. *J. Polym Sci.: Part A: Polym Chem* **2004**, *42*, 3285–3292. (d) Sharma, R.; Goyal, A.; Caruthers, J. M.; Won, Y. *Macromolecules* **2006**, *39*, 4680–4689. (e) Roos, S. G.; Mueller, A. H. E.; Matyjaszewski, K. *Macromolecules* **1999**, *32*, 8331–8335.

(9) Matyjaszewski, K. *Macromolecules* **1998**, *31*, 4710–4717.

(10) Ahmad, N. M.; Charleux, B.; Farcet, C.; Ferguson, C. J.; Gaynor, S. G.; Hawkett, B. S.; Heatley, F.; Klumperman, B.; Konkolewicz, D.; Lovell, P. A.; Matyjaszewski, K.; Venkatesh, R. *Macromol. Rapid Commun.* **2009**, *30*, 2002–2021.

(11) Reyes, Y.; Asua, J. M. *Macromol. Rapid Commun.* **2011**, *32*, 63–67.

(12) McLeish, T. C. B.; Larson, R. G. *J. Rheol.* **1998**, *42*, 81–110.

(13) (a) Axelson, D. E.; Mandelkern, L.; Levy, G. C. *Macromolecules* **1977**, *10*, 557–558. (b) Axelson, D. E.; Levy, G. C.; Mandelkern, L. *Macromolecules* **1979**, *12*, 41–52. (c) Cavagna, F. *Macromolecules* **1981**, *14*, 215–216. (d) Usami, T.; Takayama, S. *Macromolecules* **1984**, *17*, 1756–1761. (e) Bugada, D. C.; Rudin, A. *J. Appl. Polym. Sci.* **1987**, *33*, 87–93. (f) Liu, W.; Ray, D. G.; Rinaldi, P. L. *Macromolecules* **1999**, *32*, 3817–3819. (g) Shroff, R. N.; Mavridis, H. *Macromolecules* **2001**, *34*, 7362–7367. (h) Yu, Y.; DesLauriers, P. J.; Rohlfing, D. C. *Polymer* **2005**, *46*, 5165–5182. (i) Pollard, M.; Klimke, K.; Graf, R.; Spiess, H. W.; Wilhelm, M.; Sperber, O.; Piel, C.; Kaminsky, W. *Macromolecules* **2004**, *37*, 813–825.

(14) Ahmad, N. M.; Heatley, F.; Lovell, P. A. *Macromolecules* **1998**, *31*, 2822–2827.

(15) Shroff, R. N.; Mavridis, H. *Macromolecules* **1999**, *32*, 8454–8464.

(16) Parkinson, M.; Klimke, K.; Spiess, H. W.; Wilhelm, M. *Macromol. Chem. Phys.* **2007**, *208*, 2128–2133.

(17) Castignolles, P.; Graf, R.; Parkinson, M.; Wilhelm, M.; Gaborieau, M. *Polymer* **2009**, *50*, 2373–2383.

(18) Wood-Adams, P. M.; Dealy, J. M. *Macromolecules* **2000**, *33*, 7481–7488.

(19) (a) Podzimek, S.; Vlcek, T.; Johann, C. *J. Appl. Polym. Sci.* **2001**, *81*, 1588–1594. (b) Podzimek, S.; Vlcek, T. *J. Appl. Polym. Sci.* **2001**, *82*, 454–460. (c) Gaborieau, M.; Nicolas, J.; Save, M.; Charleux, B.; Vairon, J.-P.; Gilbert, R. G.; Castignolles, P. *J. Chromatogr. A* **2008**, *1190*, 215–223.

(20) Sheiko, S. S.; da Silva, M.; Shirvaniants, D.; LaRue, I.; Prokhorova, S.; Moeller, M.; Beers, K.; Matyjaszewski, K. *J. Am. Chem. Soc.* **2003**, *125*, 6725–6728.

(21) (a) Rivetti, C.; Guthold, M.; Bustamante, C. *J. Mol. Biol.* **1996**, *264*, 919–932. (b) LaRue, I.; Adam, M.; Silva, M. d.; Sheiko, S. S.; Rubinstein, M. *Macromolecules* **2004**, *37*, 5002–5005. (c) Boyce, J. R.; Shirvanyants, D.; Sheiko, S. S.; Ivanov, D. A.; Qin, S.; Boerner, H.; Matyjaszewski, K. *Langmuir* **2004**, *20*, 6005–6011.

(22) (a) Sheiko, S. S.; Prokhorova, S. A.; Beers, K. L.; Matyjaszewski, K.; Potemkin, I. I.; Khokhlov, A. R.; Moeller, M. *Macromolecules* **2001**, *34*, 8354–8360. (b) Kumaki, J.; Hashimoto, T. *J. Am. Chem. Soc.* **2003**, *125*, 4907–4917. (c) Gallyamov, M. O.; Tartsch, B.; Khokhlov, A. R.; Sheiko, S. S.; Börner, H. G.; Matyjaszewski, K.; Möller, M. *Macromol. Rapid Commun.* **2004**, *25*, 1703–1707. (d) Roiter, Y.; Minko, S. *J. Am. Chem. Soc.* **2005**, *127*, 15688–15689. (e) Schappacher, M.; Deffieux, A. *Macromolecules* **2005**, *38*, 4942–4946. (f) Kasëmi, E.; Zhuang, W.; Rabe, J. P.; Fischer, K.; Schmidt, M.; Colussi, M.; Keul, H.; D. Yi, H. C.; Schlüter, A. D. *J. Am. Chem. Soc.* **2006**, *128*, 5091–5099.

(23) Qin, S.; Matyjaszewski, K.; Xu, H.; Sheiko, S. S. *Macromolecules* **2003**, *36*, 605–612.

(24) Kreutzer, G.; Ternat, C.; Nguyen, T. Q.; Plummer, C. J. G.; Månson, J.-E.; Castelletto, V.; Hamley, I. W.; Sun, F.; Sheiko, S. S.; Klok, H. *Macromolecules* **2006**, *39*, 4507–4516.

(25) Kiriy, A.; Gorodyska, G.; Kiriy, N.; Sheparovych, R.; Lupytsky, R.; Minko, S.; Stamm, M. *Macromolecules* **2005**, *38*, 501–506.
(26) Kuhlman, W. A.; Olivetti, E. A.; Griffith, L. G.; Mayes, A. M. *Macromolecules* **2006**, *39*, 5122–5126.
(27) Brandrup, J.; Immergut, E. H.; Grulke, E. A. In *Polymer handbook*; Wiley: New York, 1999.
(28) Matyjaszewski, K.; Spanswick, J. *Mater. Today* **2005**, *8*, 26–33.
(29) (a) Wegrzyn, J. K.; Stephan, T.; Lau, R.; Grubbs, R. B. *J. Polym. Sci, Part A: Polym. Chem.* **2005**, *43*, 2977–2984. (b) Mes, E. P. C.; de Jonge, H.; Klein, T.; Welz, R. R.; Gillespie, D. T. *J. Chromatogr. A* **2007**, *1154*, 319–330. (c) Mourey, T. H. *Int. J. Polym. Anal. Charact.* **2004**, *9*, 97–135. (d) Quirk, R. P.; Lee, B. *Polym. Int.* **1992**, *27*, 359–367.
(30) (a) Chiefari, J.; Jeffery, J.; Mayadunne, R.; Moad, G.; Rizzardo, E.; Thang, S. H. *Macromolecules* **1999**, *32*, 7700–7702. (b) Yamada, B.; Azukizawa, M.; Yamazoe, H.; Hill, D. J. T.; Pomery, P. J. *Polymer* **2000**, *41*, 5611–5618. (c) Azukizawa, M.; Yamada, B.; Hill, D. J. T.; Pomery, P. J. *Macromol. Chem. Phys.* **2000**, *201*, 774–781. (d) Hirano, T.; Yamada, B. *Polymer* **2003**, *44*, 347–354. (e) Plessis, C.; Arzamendi, G.; Leiza, J. R.; Schoonbrood, H. A. S.; Charmot, D.; Asua, J. M. *Macromolecules* **2000**, *33*, 4–7. (f) Plessis, C.; Arzamendi, G.; Alberdi, J. M.; Agnely, M.; Leiza, J. R.; Asua, J. M. *Macromolecules* **2001**, *34*, 6138–6143. (g) Grady, M. C.; Simonsick, W. J.; Hutchinson, R. A. *Macromol. Symp.* **2002**, *182*, 149–168. (h) Heatley, F.; Lovell, P. A.; Yamashita, T. *Macromolecules* **2001**, *34*, 7636–7641.
(31) Rubinstein, M.; Colby, R. H. In *Polymer physics*; Oxford University Press: Oxford, U.K., and New York, 2003; p 440.
(32) Panyukov, S.; Zhulina, E. B.; Sheiko, S. S.; Randall, G.; Brock, J.; Rubinstein, M. *J. Phys. Chem. B* **2009**, *113*, 3750–3768.
(33) Sun, F. C.; Dobrynin, A. V.; Shirvanyants, D.; Lee, H.; Matyjaszewski, K.; Rubinstein, G. J.; Rubinstein, M.; Sheiko, S. S. *Phys. Rev. Lett.* **2007**, *99*, 137801.
(34) (a) Stevens, M. P. In *Polymer Chemistry: An Introduction*; Oxford University Press: Oxford, U.K., and New York, 1999; (b) Peck, A.; Hutchinson, R. A. *Macromolecules* **2004**, *37*, 5944–5951.